Supplementary Information (SI) for EES Batteries.
This journal is © The Royal Society of Chemistry 2026

Supplementary Information

Common-Ion Driven Self-Assembly of Cu Nanoparticles for Interfacial Stabilization of Zn Anodes

Jooyoung Jang, [a] *Yeonwoo Jeong* [b] *and Changshin Jo** [a, b]

[a] Department of Battery Engineering, Graduate Institute of Ferrous & Eco Materials Technology, Pohang University of Science and Technology (POSTECH), 77 Cheongam-ro, Nam-gu, Pohang, Gyeongbuk, 37673, Republic of Korea
E-mail: jochangshin@postech.ac.kr

[b] Department of Chemical Engineering, Pohang University of Science and Technology (POSTECH), 77 Cheongam-ro, Nam-gu, Pohang, Gyeongbuk, 37673, Republic of Korea

Experimental Section

Materials

Copper(II) sulfate ($CuSO_4$, Sigma-Aldrich), Zinc sulfate heptahydrate ($ZnSO_4 \cdot 7H_2O$, Alfa Aesar), Vanadium(V) oxide (V_2O_5, Sigma Aldrich), Sodium chloride (NaCl, SAMCHUN CHEMICALS), Super C (MTI Korea), Poly(vinylidene fluoride) (PVdF, Sigma-Aldrich), 1-mehtyl-2-pyrrolidinone (NMP, Sigma-Aldrich), All powders were used without further purification. Deionized water (DI-water) was purified by a HIQ III water purifier.

Preparation of Cu coating electrodes

Zn metal foil (16 mm in diameter) was cut into circular disks and used as substrates for surface modification. For the CS condition, the Zn disks were immersed in 4 mL of 0.05 M $CuSO_4$ aqueous solution for 30 s, during which spontaneous galvanic replacement occurred between Zn and Cu^{2+}, leading to the deposition of Cu particles on the Zn surface. For the ZSCS condition, the same procedure was carried out in a mixed solution containing 0.05 M $CuSO_4$ and 1 M $ZnSO_4$. To investigate the effect of $CuSO_4$ concentration, additional tests were conducted in 1 M $ZnSO_4$ solutions containing 0.01 M and 0.1 M $CuSO_4$. After immersion, the electrodes were thoroughly rinsed with deionized water and dried under vacuum before electrochemical testing. Bare Zn disks without surface modification were used as control samples.

Material Characterization

The morphology of the electrodes was examined using Atomic Force Microscope (AFM, Jupiter XR) and Scanning electron microscopy (SEM, JEOL, JSM-7900F) equipped with energy-dispersive X-ray spectroscopy (EDS) to confirm elemental distribution. Transmission electron microscopy (TEM, JEOL, JEM-2100F) was employed to further investigate the surface

characteristics of the Cu nanoparticles. X-ray diffraction (XRD, Bruker, D8-Advance Davinci) patterns was used to identify crystalline phases and to evaluate possible byproduct formation after electrode immersion. X-ray photoelectron spectroscopy (XPS, Thermo Scientific ESCALAB 250) was performed to analyze the chemical states of the samples. Fourier transform infrared (FTIR) spectroscopy (Perkin Elmer Model Spectrum Two) was carried out to study the hydrogen-bonding network of the solutions. Contact angle measurements were conducted to assess electrolyte wettability of electrode surfaces.

Synthesis of Sodium vanadate (NVO) materials

2.5 g of V_2O_5 powder was mixed in 50 mL of 2 M NaCl aqueous solution and subjected to sonication for 1 h, followed by continuous stirring at 25 °C for 4 days. The product was collected by centrifugation, repeatedly washed with deionized water and ethanol, and dried at 70 °C for 24 h, yielding sodium vanadate (NVO) nanofiber powder.

Preparation of NVO electrodes

The NVO electrodes were fabricated via a conventional slurry-casting process. The slurry was composed of NVO as the active material, Super C as the conductive additive, and PVdF as the binder in a weight ratio of 7:2:1, using NMP as the solvent. The resulting slurry was coated onto stainless steel foil and subsequently dried in a vacuum oven at 70 °C for 12 h. The dried electrodes were then punched into circular disks (10 mm in diameter) with an active material loading of 2.0 $\pm$ 0.5 mg cm^{-2}.

Electrochemical characterization

CR2032-type coin cells were assembled for electrochemical measurements. The Zn anode was prepared by punching 16 mm diameter disks from Zn foil, while GF/A glass fiber was employed as the separator. The electrolyte consisted of 2 M $ZnSO_4$ aqueous solution prepared with deionized water as the solvent. 100 µL of electrolyte added into the cell before the cell was crimped. All the electrochemical tests were performed using a WBCS3000L (WonAtech) cell test system.

Zn||Zn symmetric and Zn||Cu asymmetric cell configurations were fabricated and tested with various current densities and areal capacitie to evaluate the plating/stripping behavior and interfacial stability of Zn electrodes. Chronoamperometry (CA) measurements with Zn||Zn symmetric cell configuration were conducted at a constant overpotential of −150 mV to monitor Zn nucleation and growth dynamics. For rate test, Zn symmetric cells were tested with capacity of 1 mA h cm^{-2} with different current densities (0.5, 1, 2, 5, and 10 mA cm^{-2}) for each 10 cycles.

Electrochemical impedance spectroscopy (EIS) test was used to measure charge transfer resistance of Zn symmetric cells from Nyquist plot. Impedance measurements were carried out between 10 kHz to 0.02 Hz with an AC amplitude of 10 mV using a ZIVE MP1 (WonAtech Co., Korea) workstation.

The hydrogen evolution reaction (HER) was evaluated using linear sweep voltammetry (LSV) in a three-electrode configuration. Bare Zn, CS, ZSCS electrodes were used as the working electrodes, Bare Zn electrode served as the counter electrode, and Ag/AgCl was employed as the reference electrode. The measurements were carried out in 2 M Na_2SO_4 aqueous electrolyte at a scan rate of 1 mV s^{-1}

For ex situ SEM analysis of Zn electrodes, the Zn symmetric and asymmetric cells and full-cells were fabricated and tested with varying current densities and areal capacities. After Zn

stripping and plating process, the electrodes were treated as follows: The cycled coin cell was disassembled, and the electrode was rinsed with DI water two times and dried. Subsequently, the electrode was attached to the SEM mount using carbon tape, and top-view SEM images were obtained.

To observe initial deposition morphologies, the Zn||Cu cells were passed through a single deposition process at a current density of 1 mA cm^{-2} for 30- and 60 minutes. Moreover, Zn symmetric cells were tested for 20 and 100 cycles to determine the Zn deposition behavior at deep cycling of 1 mA cm^{-2} with 1 mA h cm^{-2}.

Cyclic voltammetry (CV) tests of the full cells were carried out in a potential window 0.2–1.6 V vs. Zn^{2+}/Zn at scan rate of 0.2 mV s^{-1}. Galvanostatic charge/discharge (GCD) test was used to investigate the reversibility of Zn^{2+} storage ability of NVO electrode. All cells in this paper was cycled at 200 A g^{-1} and 1 A g^{-1}. The charge cut-off voltage was set to 1.6 V, while discharge cut-off voltage was identical to 0.2 V for all tests. The in-situ XRD measurments were conducted at the 5A-MS-XRS beamline of Pohang Accelerator Laboratory (PAL), Korea.

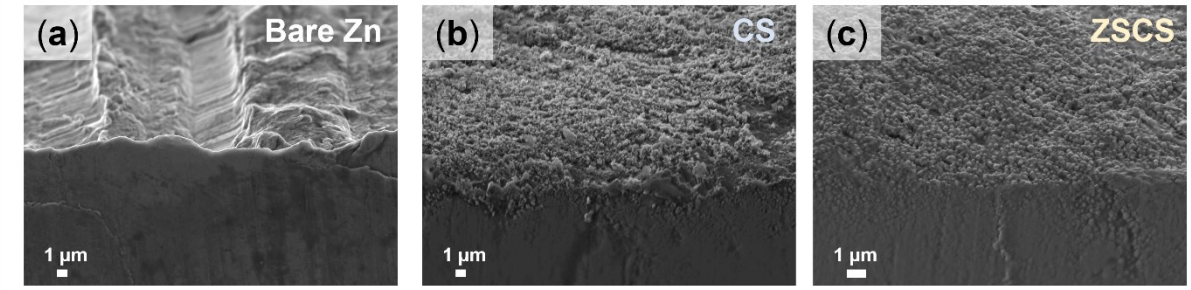

Fig. S1 Cross-sectional SEM images of (a) bare Zn and Zn electrodes after surface modification: (b) CS and (c) ZSCS.

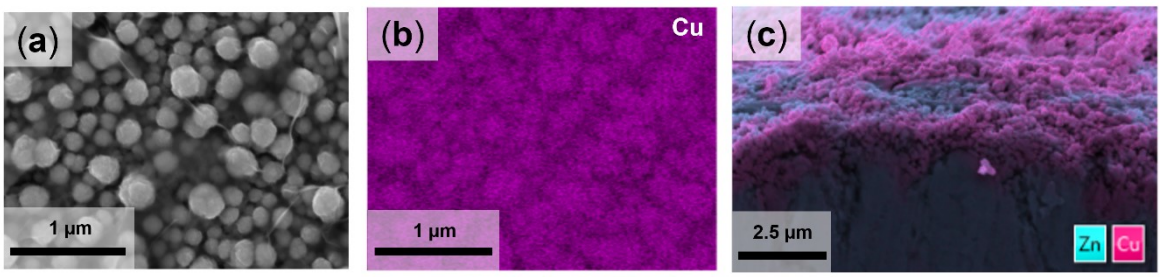

Fig. S2 (a) Top-view SEM image, (b) corresponding EDS elemental mapping, and (c) cross-sectional EDS mapping of the ZSCS-treated Zn electrode.

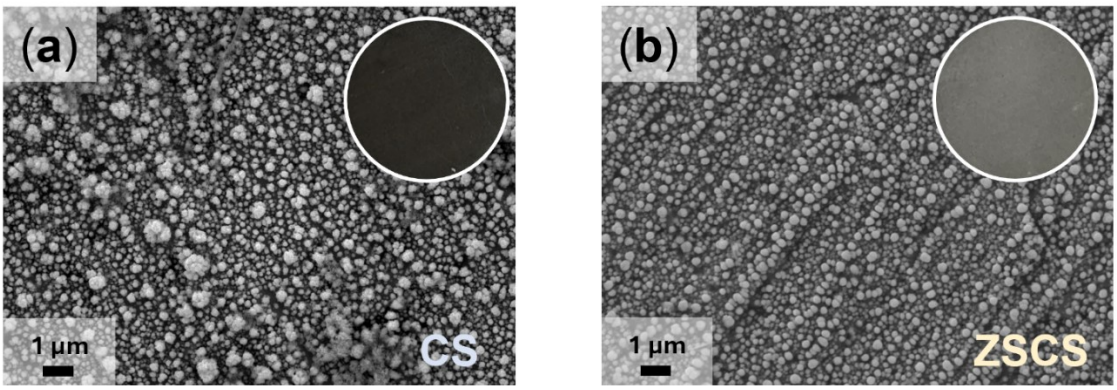

Fig. S3 Low-magnification top-view SEM images of Zn electrodes: (a) CS and (b) ZSCS (insets: corresponding photographs of the CS and ZSCS electrodes).

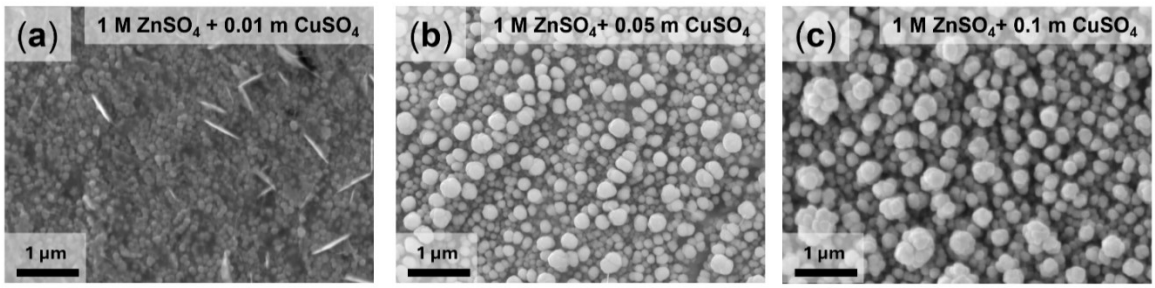

Fig. S4 Top-view SEM images of Cu particles deposited under varying $CuSO_4$ concentrations.

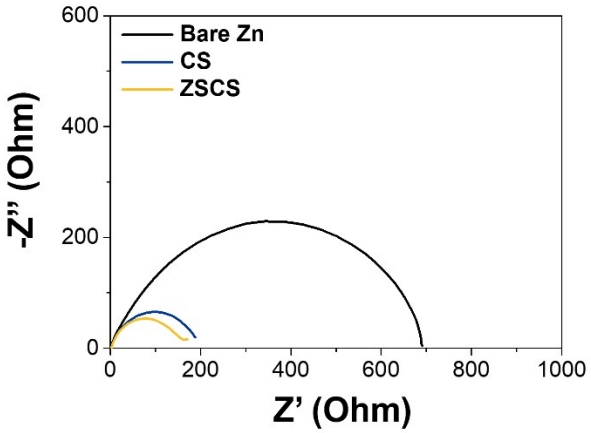

Fig. S5 Electrochemical impedance spectroscopy (EIS) spectra of Zn symmetric cells after 6 h of rest.

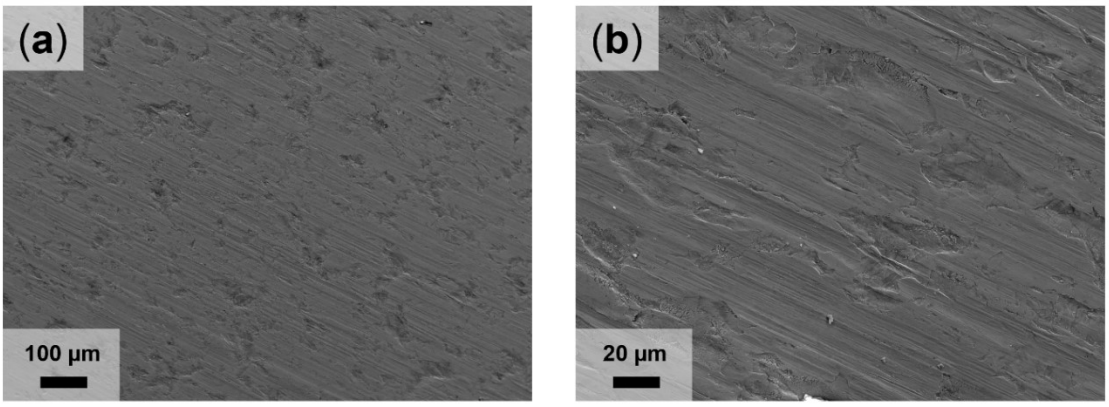

Fig. S6 Top-view SEM images of Zn electrodes at two different magnifications: (a) low magnification and (b) high magnification.

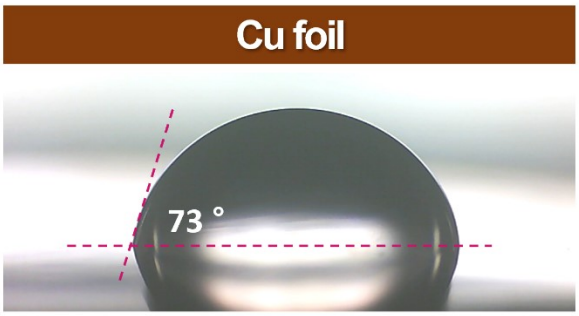

Fig. S7 Contact angle measurements of Cu foil using 2 M $ZnSO_4$.

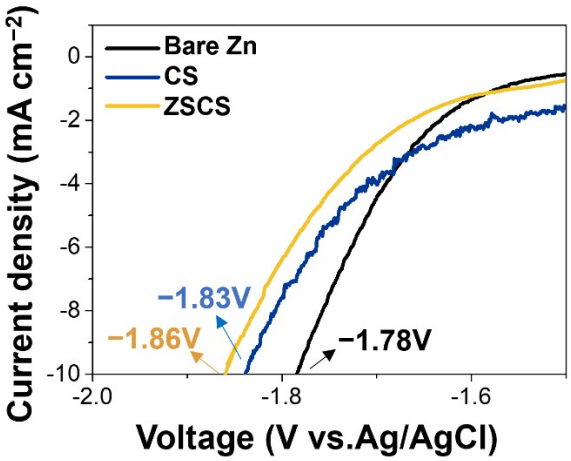

Fig. S8 Linear sweep voltammetry (LSV) curves for hydrogen evolution reaction on bare Zn, CS, and ZSCS electrodes in 2 M Na_2SO_4.

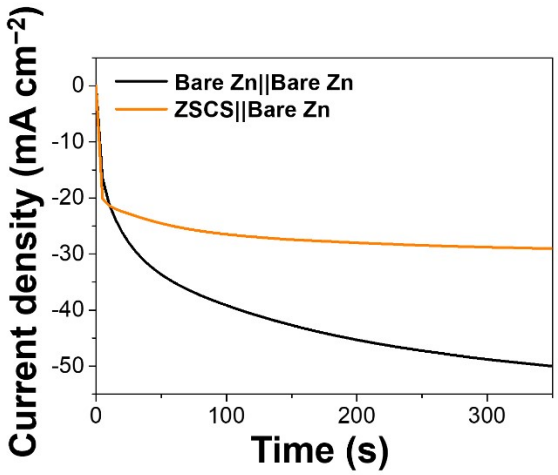

Fig. S9 Chronoamperometry results of Zn||Zn symmetric cells under a constant overpotential of −150 mV.

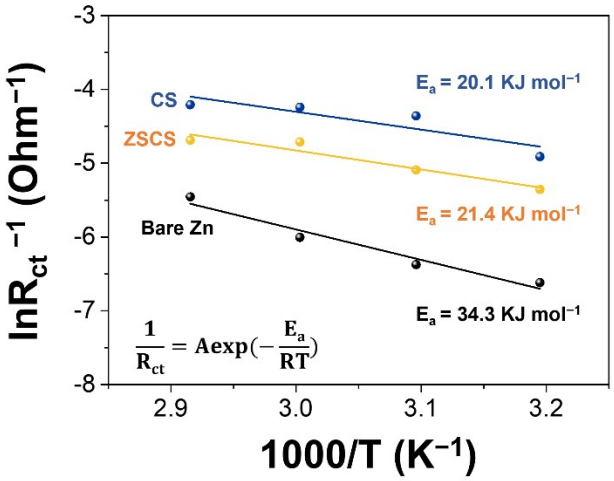

Fig. S10 Activation energy (Ea) calculated from Arrhenius plots of Zn||Zn symmetric cells with bare Zn, CS, and ZSCS electrodes.

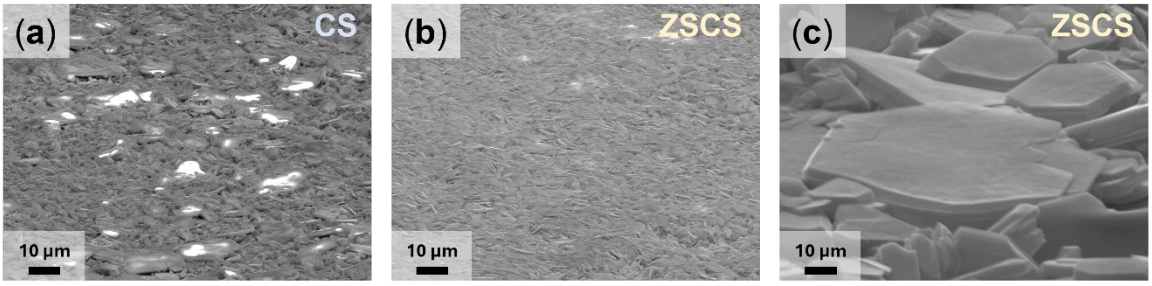

Fig. S11 70° tilted-view SEM images showing Zn deposition morphology after 100 cycles (1 mA cm^{-2} with 1 mA h cm^{-2}): (a) CS, (b) ZSCS, and (c) high-magnification view of ZSCS.

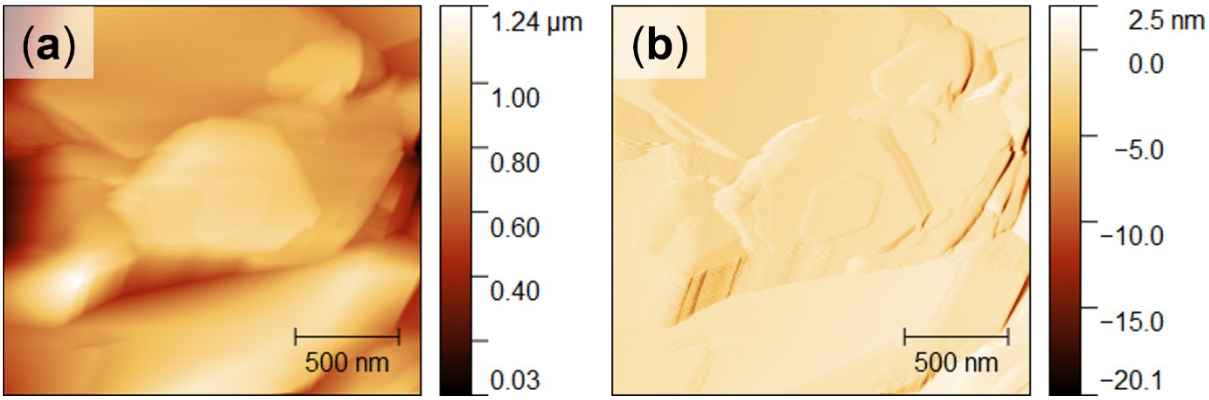

Fig. S12 Atomic force microscopy images of the ZSCS electrode after 100 cycles at 1 mA cm^{-2} with an areal capacity of 1 mA h cm^{-2}: (a) height image and (b) amplitude image.

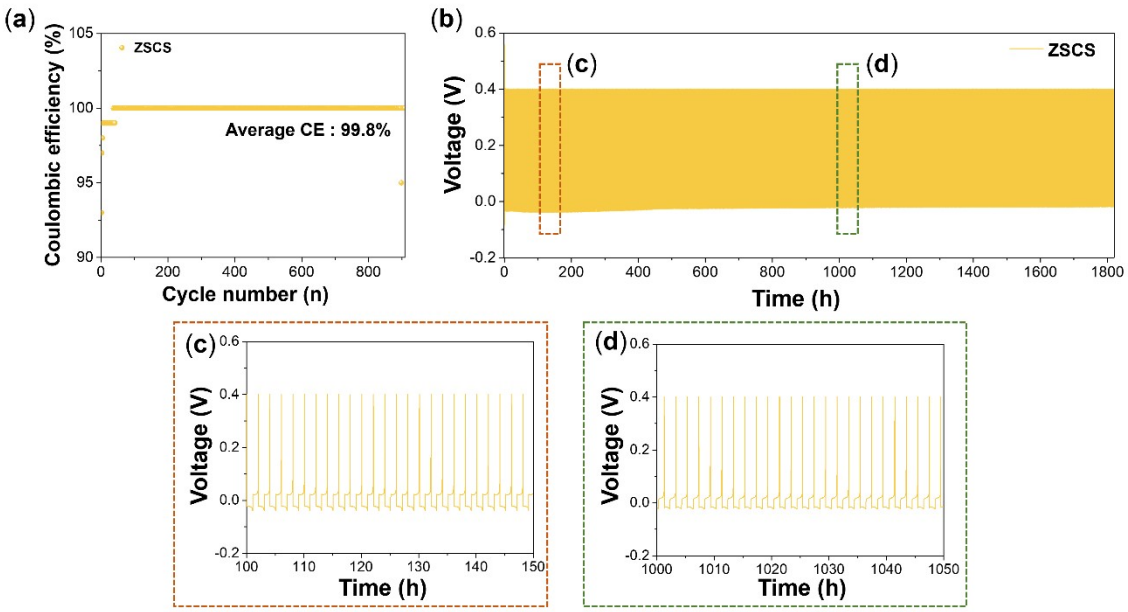

Fig. S13 (a) Coulombic efficiency of the Zn||Cu cell with a ZSCS electrode. (b) Voltage profiles of the Zn||Cu cell with ZSCS electrode during cycling. (c) Enlarged view of the voltage profiles from 100–150 h, and (d) from 1000–1050 h, corresponding to the regions highlighted in (b).

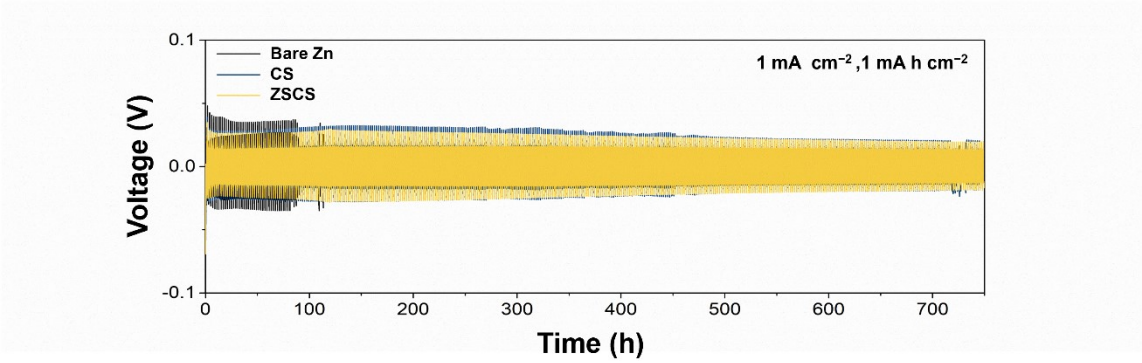

Fig. S14 Voltage profiles of Zn||Zn symmetric cells obtained at 1 mA cm^{-2} with an areal capacity of 1 mA h cm^{-2}.

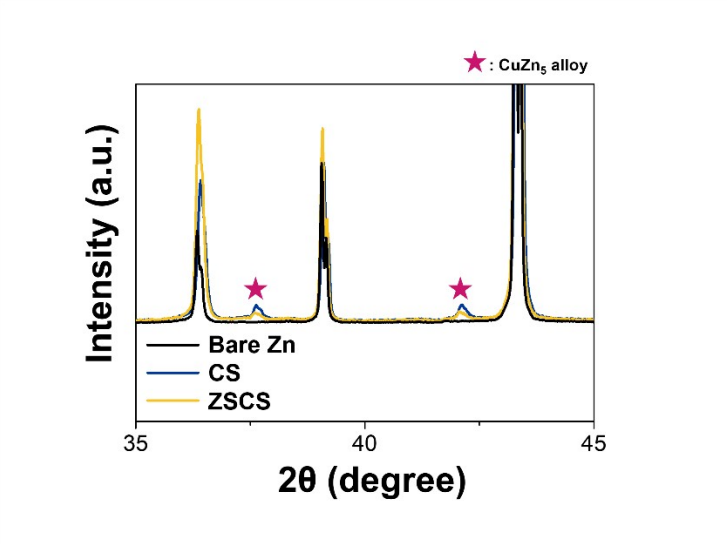

Fig. S15 Enlarged XRD patterns (from Fig. 4f) of bare Zn, CS, and ZSCS electrodes after 20 cycles, highlighting $CuZn_5$-related peaks in the Cu-modified electrodes.

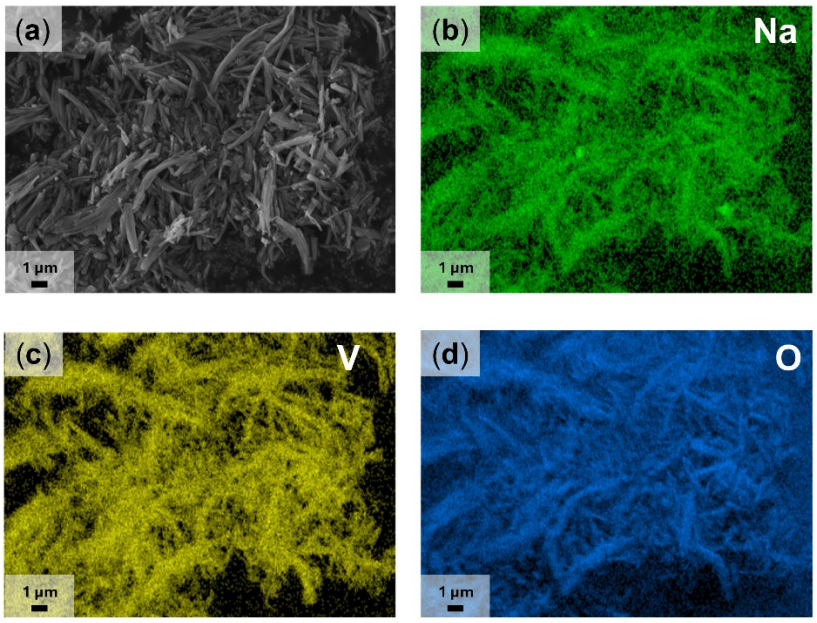

Fig. S16 (a) SEM image of NVO powder. (b–d) Corresponding EDS elemental mapping images for (b) Na, (c) V, and (d) O.

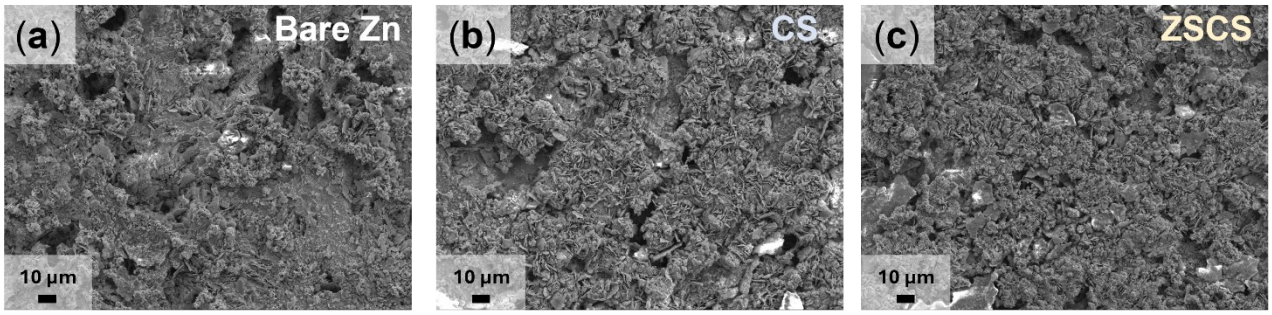

Fig. S17 ex situ SEM images of Zn anodes from NVO full-cells after 100 cycles at 1 A g^{-1}: (a) bare Zn, (b) CS, and (c) ZSCS electrodes.